Generalized Belief Propagation Detector for TDMR Microcell Model

Seyed Mehrdad Khatami, and Bane Vasić
ECE Department, University of Arizona , Tucson, AZ, 85721, USA
Email: {khatami,vasic}@ece.arizona.edu

***Abstract*—Signal processing in TDMR encounters several challenges such as read channel modeling and detection in the presence of severe two-dimensional inter-symbol interference (2-D ISI). The contribution of this paper is twofold: 1) In this paper, we introduce a novel 2-D read channel model which we call the 2-D Microcell model. In this model, we use generalized 2-D microtracks called microcells to captures the properties of irregular grain boundaries of the medium in a relatively simple yet accurate manner. The data dependent noise (DDN) distributions are analytically derived for this model. The derivation of the DDN distributions makes the 2-D Microcell suitable for detector design purposes. 2) We propose a new framework for designing truly two-dimensional detectors for the Microcell model based on near-optimal generalized belief propagation (GBP). The GBP algorithm is purposefully applied for detection in this model in order to handle the data dependent media noise which is caused by irregular bit transitions in both dimensions. Results are provided to show that the incorporation of the DDN distributions into the GBP detection helps improving the detection performance.**

***Index Terms*— Two dimensional magnetic recording (TDMR), Generalized belief propagation (GBP), 2-D microcell model, Inter symbol interference (ISI), Data dependent noise**

I. Introduction

As a new magnetic recording paradigm, TDMR aims to record one bit of information in one or a few grains, with the goal of achieving a recording density of 10 $\mathrm{Tb/in}^2$ [1]. Signal processing in TDMR encounters several challenges such as read channel modeling, detection in the presence of severe two-dimensional inter-symbol interference (2-D ISI), constrained and error correction code design and etc. Among these, modeling of the read channel is one of the critical issues for detector design.

TDMR channel models have been studied in [2]. Since most of these models such as micromagnetic [3], discrete-grain [4] and binary error and erasure channel (BEEC) model are unable to produce the data dependent noise (DDN) distributions, they are not suited for detector design. In case of Voronoi model, it is too complex to derive the DDN properties analytically for the detector design. In this paper, we consider densities which the bit to grain size ratio is of the order of $5-10$. The 2-D Microcell model is the generalization of the traditional Microtrack model [5] to two dimensions so that each bit is composed of a small number of horizontal and vertical tracks. It is an accurate and relatively simple model that captures the properties of irregular grain boundaries at these densities. This model enables the analytical derivation of the pattern dependent distributions of the read-head output samples. The resulting channel is a 2-D ISI channel in which noise depends on the input data pattern as well as on the random realization of microcells.

There have been several important works on 2-D detection for ISI and magnetic recording channels. The core of techniques used in [6]–[10] is using 2-D equalization followed by 1-D MAP detectors in both directions. 2-D Decision Feedback Equalizer (DFE) and MAP-DFE hybrid equalization schemes is considered in [11]. In [12], separable 2-D ISI channel is used for transmission. Non-binary column MAP detector concatenated to a binary row MAP detector followed by LDPC decoder is considered.

However, all these detection schemes are multi-track rather than 2-D, and consequently cannot fully exploit the characteristics of the channel detection with 2-D interference. Furthermore, these algorithms are not compatible with DDN ISI channel. In this paper, we consider the Generalized Belief Propagation (GBP [13]) algorithm as a detection algorithm for the 2-D Microcell model. The GBP algorithm, which originates from statistical physics, has been first considered in the context of 2-D detection by Shental *et al.* [14]. Using GBP is a natural way of exploiting the 2-D characteristics of ISI, and in [14] it was shown that the performance of GBP is almost the same as maximum *a* posteriori (MAP) detector. Our main contribution is the formulation of the GBP algorithm for 2-D detection in 2-D Microcell model. Unlike [14], the read-head output samples are contaminated by the data dependent media noise. Since the Microcell model allows for the exact calculation of the DDN distribution, we incorporate this into the GBP algorithm.

The paper is organized as follows: In Section II, the read channel model is introduced. The distribution of the DDN is analytically derived in Section III. Section IV outlines the detection problem. The DDN distributions are used in detection design for the modified GBP algorithm in this section. Simulation results are provided in Section IV-A. Finally, Section V concludes the paper.

II. Channel model

The read/write channel model for TDMR consists of three components: 2-D channel modeling, the data writing process and modeling the readback process. In Sections II-A and II-B, the 2-D Microcell model is introduced and the consequent DDN distributions of this modeling is analytically computed in Section III.

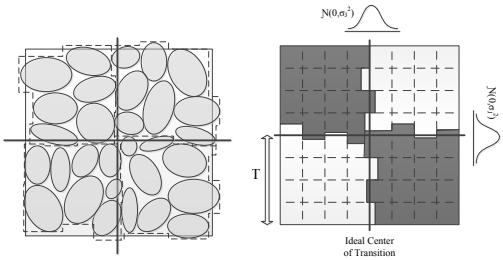

(a) (b)

Fig. 1. a) Microcell model approximation of grain boundaries by rectangles. b) 2-D Microcell model for TDMR

A. 2-D Microcell Model and Writing Process

A medium is "ideal" if the bit areas are equally sized and regularly spaced squares. We refer to the perturbed bit areas as "non-ideal cells". In a non-ideal medium, a small number of grains form one cell in which some grains straddle the cell boundaries. Fig. 1(a) shows a 2×2 non-ideal cells. Small equally sized squares represent the ideal cells. The grains which mostly lie in the ideal cell form the boundaries of the non-ideal cell. In the 2-D Microcell model, the grains which straddle the cell boundaries are modeled by small tracks displaced from the ideal cell borders. The cell on which the signal is written, is divided into N equally sized smaller tracks called microtracks which are oriented in vertical and horizontal directions. The perturbations are modeled as the random position of microtrack boundaries. A non-ideal cell with displaced transition boundaries is called a "microcell". The transition boundaries represented by a number of microtracks are independently and randomly displaced from the desired (ideal) transition position. Each shift is chosen from a distribution which is typically considered to be a truncated Gaussian distribution. Fig. 1(b) illustrates the differences between ideal cells and microcells. Through out the paper, $1/-1$ bits are colored as light/dark, respectively. We characterize the 2-D Microcell model with two parameters: the number of microtracks for a microcell in each direction N, and the boundary transition shift variance σ_J^2 [5]. T is the bit spacing and σ_J^2/T is defined as the normalized jitter variance.

The write process of the TDMR system does not have any prior knowledge of the non-ideal cell shapes and sizes in the medium. Therefore, the write head simply assumes that the medium is ideal and attempts to write in the ideal cells. The non-ideal cell which is mostly in the write area is then appropriately magnetized. Let $x_{i,j} \in \{-1, +1\}$ be the input data bits and let $x_c(t_1, t_2)$ be the continuous magnetization of the recording medium after the write process at position (t_1, t_2).

B. Readback Process

The readback signal samples are obtained by convolving the magnetization of the recording medium, $x_c(t_1, t_2)$, with the 2-D read-head response and then sampling the resulting signal at cell centers $(iT + \frac{T}{2}, jT + \frac{T}{2})$ where i, j are integers. In this paper, we assume the read-head response, $h(t_1, t_2)$, to be a truncated 2-D Gaussian pulse which spans 3×3 cells [2],

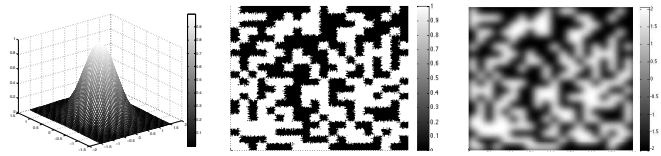

(a) (b) (c)

Fig. 2. Visualization of read channel model. a) Read-head impulse response . b) Input signal for $N = 10$ with (normalized jitter variance) $\sigma_J^2/T = 0.2$. c) Output signal after convolution of the read-head

[14]. Let $y_{i,j} \in \mathbb{R}$ be the noiseless readback signal samples and $r_{i,j} \in \mathbb{R}$ be the noisy readback signal samples. The ideal readback signal, $y_{i,j}$, can be written as:

$$y_{i,j} = \sum_{k_1=-1}^{+1} \sum_{k_2=-1}^{+1} h_{k_1,k_2} x_{i-k_1,j-k_2} \tag{1}$$

where

$$h_{k_1,k_2} = \iint_{A_{k_1,k_2}} h(\tau_1, \tau_2) d\tau_1 d\tau_2 \tag{2}$$

where A_{k_1,k_2} is the square area covering the ideal cell (k_1, k_2) in which $k_1T - \frac{T}{2} < t_1 < k_1T + \frac{T}{2}$ and $k_2T - \frac{T}{2} < t_2 < k_2T + \frac{T}{2}$. Fig 2 illustrates the read channel model for a 20×20 bits medium. Fig. 2(b) shows $x_c(t_1, t_2)$ for 2-D Microcell model. $r_{i,j}$ can be obtained by sampling the read-head output signal in Fig. 2(c) at the center of cell (i, j).

The interference is caused by the bits in the span of the read-head response. Let $C_{i,j} = \{(k_1, k_2) | i-1 \leq k_1 \leq i+1, j-1 \leq k_2 \leq j+1\}$ be the set of local neighborhood indices of bit (i, j) and $\mathbf{x}_{C_{i,j}} = \{x_{k_1,k_2} | (k_1, k_2) \in C_{i,j}\}$ be all the input data bits which contribute to the readback signal sample $r_{i,j}$. For the non-ideal case, readback samples can be rewritten as follows:

$$r_{i,j} = \sum_{k_1=-1}^{+1} \sum_{k_2=-1}^{+1} \iint_{A'_{i-k_1,j-k_2}} h(iT + \frac{T}{2} - \tau_1, jT + \frac{T}{2} - \tau_2) x_{i-k_1,j-k_2} d\tau_1 d\tau_2 \tag{3}$$

where A'_{k_1,k_2} is the area spanning the $(k_1, k_2)^{th}$ microcell. The non-ideal readback signal samples can also be written as

$$r_{i,j} = y_{i,j} + n_{i,j} \tag{4}$$

This change in output samples between the ideal and non-ideal case is considered as "media noise". $n_{i,j}$ denotes the media noise component for cell (i, j). This noise depends not only on microcell shapes in $C_{i,j}$, but on the polarity of the magnetization in the neighborhood of cell (i, j). As a result, the media noise is a data dependent and from (1), its conditional probability density function (pdf) given the local neighborhood data bits can be written as

$$p(r_{i,j} | \mathbf{x}_{C_{i,j}}) = p(r_{i,j} - y_{i,j} | \mathbf{x}_{C_{i,j}}) = p(n_{i,j} | \mathbf{x}_{C_{i,j}}) \tag{5}$$

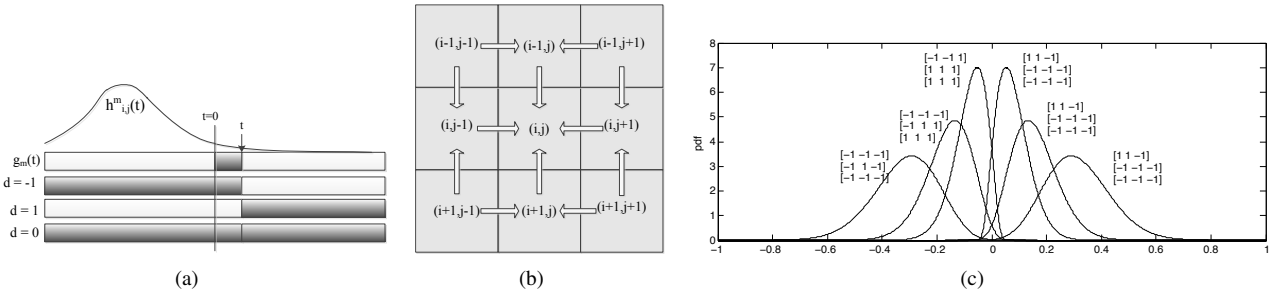

(a) (b) (c)

Fig. 3. a) $g_m(t)$ is the integral of the read-head from the ideal transition point to the random variable t. $d \in D_{i,j}$ is the coefficient for $g_m(t)$ to compute the noise component. b) The elements of $D_{i,j}$ is calculated by deducting the input data bits located at the head and the tail of the arrow. c) Data dependent media noise distributions for $N = 10$, $\sigma_J^2/T = 0.1$ for various input data patterns.

III. Data Dependent Noise Distributions

In this section, we provide a formulation for DDN distributions $p(n_{i,j}|\mathbf{x}_{C_{i,j}})$. Let $N_{i,j}$ be the set of all neighboring cells of the $(i,j)^{th}$ cell. Two cells are neighbors if they share a common side. The DDN, $n_{i,j}$, is caused by the difference between the input data for two neighboring bits in $C_{i,j}$. Therefore, $n_{i,j}$ can be broken down into a summation of smaller noise components caused by the common sides of the cells with different input data bits in $C_{i,j}$. The noise component caused by each common side can also be interpreted as a summation of noise due to each microtrack which intersects with that common side. The noise caused by each microtrack can be obtained by the integration of read-head response from the ideal transition position to the perturbed transition position in the common microtrack. The noise component introduced by the microtrack m is denoted by the random variable (RV) $g_m(t)$ where $t \sim \mathcal{N}(0, \sigma_J^2)$ is a RV of the transition position. Fig. 3(a) illustrates how the difference between two neighboring bits values cause the noise component. The parameter d can be interpreted as the sign of the noise component. The noise component of microtrack m, $g_m(t)$ is

$$g_m(t) = 2 \int_{\frac{T}{N}} \int_0^t h_{i,j}^m(\tau_1, \tau_2) d\tau_1 d\tau_2 \tag{6}$$

where $h_{i,j}^m$ is the response of the read-head over the corresponding microtrack m. We denote $D_{i,j}$ as the set of differences between the input data for two neighboring bits in $C_{i,j}$ in an order shown in Fig. 3(b).

$$D_{i,j} = \{\frac{x_{m_1,n_1} - x_{m_2,n_2}}{2} | \{(m_1,n_1),(m_2,n_2)\} \subset C_{i,j}, \tag{7}$$
$$(m_1,n_1) \in N_{m_2,n_2}, |m_1 - i| \geq |m_2 - i|, |n_1 - j| \geq |n_2 - j|\}$$

Each element of $D_{i,j}$ is assigned to one side inside the 3×3 region of the bit (i,j). The elements of $D_{i,j}$ are calculated by subtraction of two neighboring input data bits located at the head and the tail of the arrow of Fig. 3(b). Fig. 3(a) shows all values of $d \in D_{i,j}$ for the different cases of two neighboring input data bits. The total noise, $n_{i,j}$ can be written as

$$n_{i,j} = \sum_{d_k \in D_{i,j}} d_k \sum_{m=1}^{N} g_m(t) \tag{8}$$

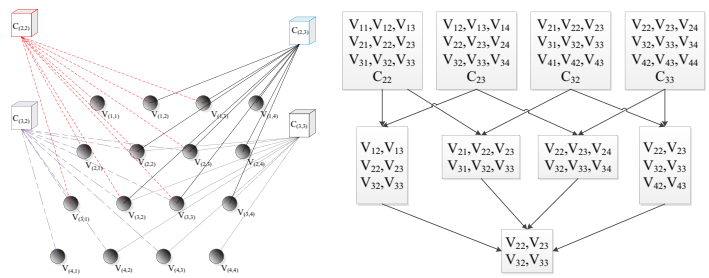

(a) (b)

Fig. 4. a) Factor graph for the 4×4 2-D ISI channel. b) A region graph generated using the cluster variation method [13].

where $d_k \sum_{m=1}^{N} g_m(t)$ is noise component caused by the common side of two neighboring bits corresponding to $d_k \in D_{i,j}$. The rest of the computations to calculate the distribution of $n_{i,j}$ is the summation of RVs according to (8), which is obtained by the convolution of the corresponding distributions. Fig. 3(c) is an example of distributions for the media noise for several input signals.

IV. GBP Detector

Finding maximum *a* posteriori solution for 2-D ISI channels is intractable for the large sizes, therefore one must resort to approximate inference methods such as message passing algorithms. For clarity, the detection method is explained through an example. This example will be used through the remainder of the paper. Let us consider a 4×4 cell square and assume that the read-head response spreads over 3×3 cells. The factor graph of our example is depicted in Fig. 4(a). Variable nodes, denoted by $V_{i,j}$, are shown as circles and factor nodes, denoted by $f_{C_{i,j}}$, as cubes with an edge connecting a variable node $V_{i,j}$ to a factor node $f_{C_{i,j}}$ if and only if $V_{i,j}$ is an argument of $f_{C_{i,j}}$. As it is shown in Fig. 4(a), there exists many cycles in 2-D ISI channel factor graph in contrast to the sparse graphs of LDPC codes. As a result, the tree-like assumption used in BP does not hold and BP approximation is poor. GBP algorithm can be used to resolve this issue.

The GBP uses region graph method to specify regions and messages. The first step in region graph method is to define the basic regions, which cover the whole graph and include all the variable nodes, which are connected to the factor node included in the region. In [13], Yedidia *et al.* explain how

to choose the appropriate regions. Next we construct a set with all primary regions, intersections of primary regions, intersections of intersections and so on. Then graphical model can be constructed using this set. A clear choice of overlapping regions is 3×3 square since this size of region is small enough to do the exact inference with not much computational complexity and large enough to contain the shortest cycles in factor graph. Fig. 4(b) is an example of a region graph for the 4×4 two-dimensional ISI channel problem.

For the formulation of GBP, we use the parent to child algorithm. In this method, we only have one kind of message, which is message from parent to child. The arrows in Fig. 4(b) which connect parent regions to child regions are the messages for our example. For the message-update rules in the parent-to-child algorithm, see [13].

The major advantage of GBP is benefiting from region to region message passing instead of node to node message passing. By selecting 3×3 squares as the regions in GBP, DDN distributions can be applied in calculating $f_{C_{i,j}}$ to improve the performance of the detector. The DDN distributions are calculated analytically in Section II-B (Fig. 3(c)).

To make the computations tractable, the DDN distributions are approximated by Gaussian distributions. Mean and variance of Gaussian distributions are set to mean and variance of the computed distributions for each state of the input. Therefore the computational complexity of distribution adjusted GBP (DAGBP) and Conventional GBP (CGBP) are exactly the same by the Gaussian approximation.

A. Comparison of GBP detectors

Although GBP is more complex than the previous works on detector design, it achieves near maximum likelihood (ML) performance for 2-D ISI channels. Therefore, the purpose of this section is not to compare GBP with other detectors, but to illustrate how the incorporation of DDN distributions can improve GBP. In this section, the performance of the CGBP and DAGBP detectors are evaluated for 2-D ISI channel using Monte Carlo simulations. We simulated a 8×8 cell two-dimensional channel. The symbols were assumed to have known value in marginal cells of the grid. Fig. 5 compares the CGBP and DAGBP performance in terms of BER as a function of SNR_w for different values of media jitter (σ_J^2/T). As it is shown, the performance improvement for $\sigma_J^2/T = 0.2$ is about $2dB$ and $1dB$ for $\sigma_J^2/T = 0.1$. The number of microtracks in each microcell is set to $N = 10$.

V. Conclusion

In this paper, we generalized the notion of microtrack modeling for TDMR. 2-D Microcell model is explained in details as an accurate and relatively simple read channel model. The data dependent media noise distributions are calculated for this read channel model. Taking these distributions into account, GBP is modified to match the specific problem. Since GBP can work with cluster of nodes, it can work with locally data dependent media noise distributions to improve the performance.

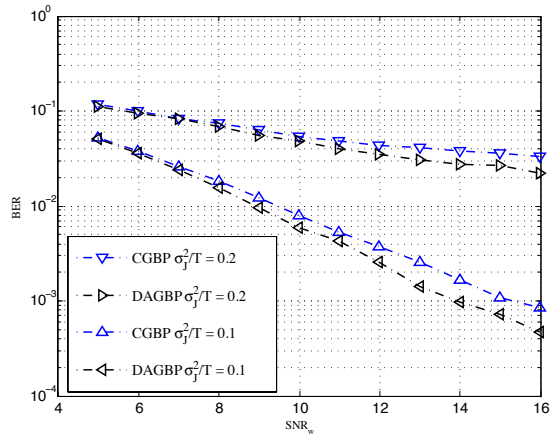

Fig. 5. Comparison of CGBP and DAGBP for different σ_J^2/T

Acknowledgment

This work is funded by IDEMA ASTC and partially by NSF under Grant CCF-0963726. The authors would like to thank Anantha Raman Krishnan and Shayan Srinivasa Garani for their helpful suggestions.

References

[1] R. Wood, M. Williams, A. Kavcic, and J. Miles, "The feasibility of magnetic recording at 10 terabits per square inch on conventional media," *IEEE Trans. on Magn.*, vol. 45, no. 2, pp. 917 –923, Feb. 2009.

[2] A. Krishnan, R. Radhakrishnan, B. Vasic, A. Kavcic, W. Ryan, and F. Erden, "2-d magnetic recording: Read channel modeling and detection," *IEEE Trans. on Magn.*, vol. 45, no. 10, pp. 3830 –3836, Oct. 2009.

[3] K. S. Chan, J. Miles, E. Hwang, B. VijayaKumar, J.-G. Zhu, W.-C. Lin, and R. Negi, "Tdmr platform simulations and experiments," *IEEE Trans. on Magn.*, vol. 45, no. 10, pp. 3837 –3843, Oct. 2009.

[4] A. Kavcic, X. Huang, B. Vasic, W. Ryan, and M. Erden, "Channel modeling and capacity bounds for two-dimensional magnetic recording," *Magnetics, IEEE Transactions on*, vol. 46, no. 3, pp. 812 –818, march 2010.

[5] C. Modlin, K. Fisher, and J. Cioffi, "Analysis of and detector comparisons using the microtrack model of magnetic recording," *IEEE Trans. on Magn.*, vol. 34, no. 1, pp. 63 –68, Jan. 1998.

[6] S. Nabavi and B. Vijaya Kumar, "Two-dimensional generalized partial response equalizer for bit-patterned media," in *IEEE Int. Conf. on Comm., 2007. ICC '07.*, Jun. 2007, pp. 6249 –6254.

[7] S. Karakulak, P. Siegel, J. Wolf, and H. Bertram, "Joint-track equalization and detection for bit patterned media recording," *IEEE Trans. on Magn.*, vol. 46, no. 9, pp. 3639 –3647, Sep. 2010.

[8] J. Kim and J. Lee, "Iterative two-dimensional soft output viterbi algorithm for patterned media," *IEEE Trans. on Magn.*, vol. 47, no. 3, pp. 594 –597, Mar. 2011.

[9] W. Chang and J. Cruz, "Inter-track interference mitigation for bit-patterned magnetic recording," *IEEE Trans. on Magn.*, vol. 46, no. 11, pp. 3899 –3908, Nov. 2010.

[10] S. Nabavi, B. Kumar, and J.-G. Zhu, "Modifying viterbi algorithm to mitigate intertrack interference in bit-patterned media," *IEEE Trans. on Magn.*, vol. 43, no. 6, pp. 2274 –2276, Jun. 2007.

[11] M. Marrow and J. Wolf, "Iterative detection of 2-dimensional isi channels," in *Inf. Theory Workshop, 2003. Proc. 2003 IEEE*, march-4 april 2003, pp. 131 – 134.

[12] Y. Wu, J. O'Sullivan, N. Singla, and R. Indeck, "Iterative detection and decoding for separable two-dimensional intersymbol interference," *IEEE Trans. on Magn.*, vol. 39, no. 4, pp. 2115 – 2120, July 2003.

[13] J. Yedidia, W. Freeman, and Y. Weiss, "Constructing free-energy approximations and generalized belief propagation algorithms," *IEEE Trans. on Inf. Theory*, vol. 51, no. 7, pp. 2282 – 2312, Jul. 2005.

[14] O. Shental, N. Shental, S. Shamai (Shitz), I. Kanter, A. Weiss, and Y. Weiss, "Discrete-input two-dimensional gaussian channels with memory: Estimation and information rates via graphical models and statistical mechanics," *IEEE Trans. on Inf. Theory*, vol. 54, no. 4, pp. 1500 –1513, Apr. 2008.